Piezoelectric polymer based acoustic energy harvester for implantable medical devices

Jawad, Husnain; Zhang, Wei; Abbasi, Saadullah; Qing, Yajie; Sheng, Chenxu; Hu, Laigui

DOI:
10.1088/2631-8695/ad1f13

Piezoelectric polymer-based acoustic energy harvester for implantable medical devices

Husnain Jawad[1], Wei Zhang[1], Saadullah Farooq Abbasi[2], Yajie Qing[1*], Chenxu Sheng[1] and Laigui Hu[1*]
[1]Department of Micro-Nano Electronics, School of Information Science and Technology Fudan University, Shanghai, China
[2]School of Electronics and Electrical Engineering, University of Birmingham, UK

E-mail: jhusnain18@fudan.edu.cn, w_zhang19@fudan.edu.cn, S.f.abbasi@bham.ac.uk, yajieqin@fudan.edu.cn, cxcheng21@m.fudan.edu.cn and laiguihu@fudan.edu.cn

Received xxxxxx
Accepted for publication xxxxxx
Published xxxxxx

Abstract

Wireless implantable devices (WIDs) have the potential to revolutionize biomedical sensing, but their power supplies face significant challenges. Traditional energy transfer methods such as inductive and RF have limitations due to associated tissue losses. This work demonstrates a promising approach to this problem, using a flexible implantable ultrasound energy harvester (IUEH) made of biocompatible Poly (vinylidene fluoride-co-trifluoro ethylene) (P(VDF-TrFe)) free-standing film. Unlike commonly used piezoceramic devices, IUEH can be fabricated using economical solution processing methods such as spin coating. In addition, the PVDF-TrFE Ultrasound energy harvesters are rarely reported in the literature. The device performance of the polymer IUEH was investigated in air, water, and animal meat tissue, and the results show that it can generate a power output of 1.1 mW/cm^2 in meat, and 1.4 mW/cm^2 in water at 80 kHz. The device fabricated using a free-standing piezoelectric thin film, offers an optimum output that is comparable to other P(VDF-TrFe) based high-frequency devices. Additionally, its flexible design, lower costs, and biocompatibility make it a promising alternative to lead-based devices; thus, offering safety, affordability, and quick customization, while promoting minimally invasive procedures and driving innovation in medical device development.

Keywords: Acoustic; Implantable, P(VDF-TrFE), Biomedical, Polymer

1. Introduction

Implantable medical devices have witnessed extensive adoption, enhancing the quality of life for millions of patients. Notably, deep brain stimulation implants and cochlear implants have been deployed on a substantial scale, with approximately 0.15 million individuals having received deep brain stimulation implants as of 2018, as estimated by the International Neuromodulation Society (INS). Additionally, the National Institute of Health (NIH-NIDCD) recorded 0.736 million cochlear implants by 2019, underscoring the growing significance of these healthcare devices. The field has seen remarkable innovation, spanning knee pressure harvesters, advanced pacemakers, retinal implants, and closed-loop stimulation devices with real-time adjustments [1–4]. In the preceding decade, extensive research and development have been observed in this discipline across the globe[5–8]. Typically, these devices rely on subcutaneous non-rechargeable batteries for power, necessitating surgical replacements – a physically and psychologically painful process for patients. [9,10]. In response to this challenge, the exploration of wireless energy transfer methods for in-vivo implantations has gained momentum[11]. Several energy transmission techniques have been developed, categorized by their transduction mechanisms, encompassing inductive, photovoltaic, thermoelectric, triboelectric, acoustic, and radio frequency (RF) energy transfer [9][10]. A comparative analysis reveals RF, photovoltaic, and inductive methods limitations due to alignment issues, tissue penetration, and low power intensity. These methods face signal attenuation and thermal issues, restricting deep implantation. In contrast, piezoelectric-based acoustic harvesters efficiently convert bodily or external acoustic energy into electricity, offering advantages like low propagation loss (1 dB/cm/MHz), shorter wavelengths, and high-power transmission for implantable medical devices [11-13]. Importantly, acoustic power transfer aligns with FDA safety limits, set at 7200 μW/mm^2, offering optimal power density for medical applications up to 144 μW/mm^2 [14,15].

The efficiency of the energy harvester relies on multiple factors, including material selection, structural composition, and fabrication techniques. Piezoelectric materials, categorized as inorganic lead-based, inorganic lead-free, and organic polymer-based, offer varied responses to high and low-frequency stimuli. In low-frequency applications, acoustic harvesters based on PVDF-TrFE, as reported by T. Inaoka and K. K. Chow have demonstrated outputs of 23-29 μV and 3.06 V, respectively [16,17]. In applications requiring higher frequencies, L. Jiang et al. [23] examined thin PZT/epoxy 1-3 piezoelectric composites, yielding an output voltage of 0.91 Vpp in 14 mm-thick pork tissue within a frequency range of 200-500 kHz, while a different Lead-based PZT energy harvester achieved 5.8 Vpp [18,19] Another study involved the utilization of KNNS piezoelectric material with copper and gold electrodes, resulting in an output of 1.4 V at a 300 kHz frequency. Q. Shi et al. introduced a PZT-based harvester with top and bottom platinum electrodes, generating a modest 2 mV during testing in water, with signal frequencies ranging from 100 kHz to 1 MHz [20,21]. Efforts to enhance energy harvester efficiency encompass advanced fabrication techniques, exemplified by T. Maleki et al., achieving 8 V output [22] Additionally, Charthed et al. improved efficiency through geometry alterations, yielding around 1 V output [23]. Table 1 provides a detailed summary of the aforementioned harvesters. Furthermore, nanocomposite piezoresistive pressure sensors and energy harvesters have exhibited promising results. An innovative $ZnO/Ti_3C_2T_x$-based device generated 10 µW at approximately 16 kPa [24], while a nano-engineered carbon-fiber-based piezoelectric smart composite achieved voltage outputs ranging from 1.4 to 7.6 V under impact acceleration of 0.1-0.4 ms^{-2}. Additionally, a PVDF-BTO Nano-composite device demonstrated a maximum output of 4.1 V under finger-tapping conditions[24–26]. M. Sadl et al. reported an unconventional work involving multifunctional energy storage and piezoelectric properties of 0.65 Pb(Mg1/3Nb2/3)O3–0.35PbTiO3 thick films on stainless-steel substrates, offering enhanced energy storage and production capabilities, despite limited suitability for implantable applications due to factors like rigidity and non-biocompatibility [27]. Advanced material analysis conducted by Jiashi et al. involved the use of 3D equations of linear piezoelectricity to assess the impact of physical parameters on output power, with results indicating that a large dielectric constant, high electromechanical coupling factor, and low stiffness significantly contribute to output power[28]. Some organic piezoelectric polymers like P(VDF-TrFe) exhibited superior qualities for subcutaneous ultrasound transduction applications, featuring large electromechanical coupling factors k_t, high remnant polarization, and flexibility while being lead-free and biocompatible. P(VDF-TrFE) offers advantages over Piezoceramic PZT due to its lightweight, flexibility, bio-safety, lead-free nature, and low acoustic impedance (~4 MRayl). This facilitates better acoustic impedance matching with water and living tissues (~1.7 MRayl) [29,30], making it preferable for implantable devices by overcoming PZT's lead-related limitations and allowing deeper implantations [31,32]. In addition, considering the practical implementation of energy harvesters, the role of geometry, composition, and fabrication methods is significant. Previous research predominantly focused on transducer structures based on beams and nano-wires, involving costly fabrication processes and displaying fragility [33]. Conversely, thin film-based diaphragm structures offer enhanced resilience and simplicity in fabrication, making them a more viable option for practical applications [34].

This work aims to tackle crucial energy harvesting for implantable medical devices. By introducing a flexible polymer film-based Implantable Ultrasound Energy Harvester (IUEH), it overcomes the challenge of providing a safe and efficient wireless energy source. The innovative use of PVDF-TrFE at Ultrasonic frequencies for energy transfer has rarely been reported before. The fabrication process incorporates cost-effective and practical microfabrication techniques, including solution processing, Physical Vapor Deposition (PVD), and DC polarization, making it an economically viable choice for powering implantable medical devices. Through rigorous testing at ultrasound frequencies (f > 20 kHz), this IUEH achieves an impressive power output of 1.1 mW, surpassing the performance of P(VDF-TrFE) thin film-based devices. This accomplishment addresses the challenge of enhancing power generation for implantable applications, ensuring an optimal energy supply for various devices. Importantly, the power consumption of biosensing systems, typically at around 50 µW, and configurations involving data processing and transfer (10 µW to 1.5 mW) align well with the capabilities of this harvester. It is suitable for powering diverse implantable devices, such as pacemakers and muscle stimulation devices, which require approximately 5-100 µW and 4.5-21 mW, respectively, making it a versatile solution for a range of implantable applications [5]. Further details are summarized in Table 1.

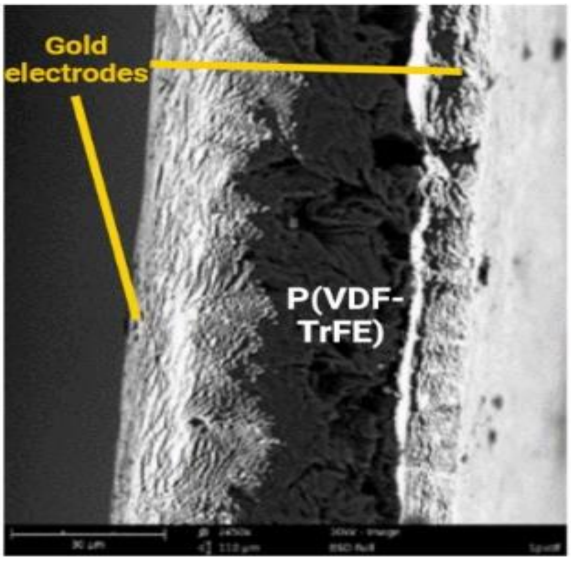

Figure 1. SEM Image

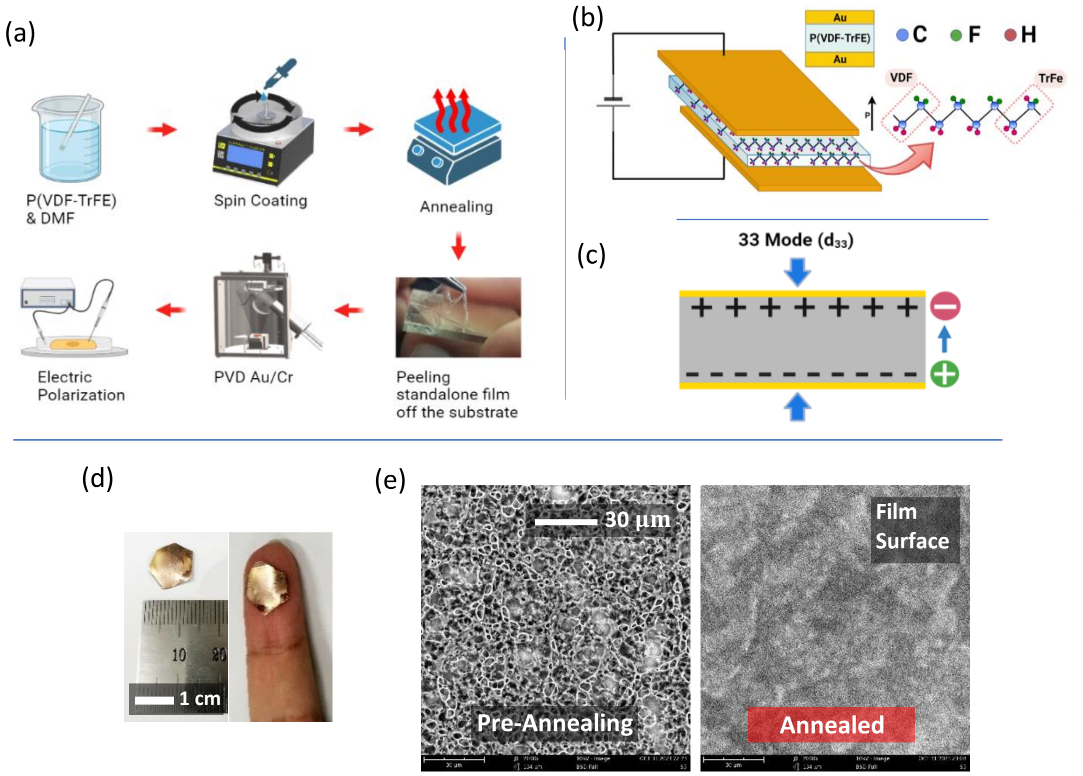

Figure 2. (a) Fabrication process of PVDF-TrFE energy harvester (b) Geometry and composition (c) Poling direction (d)The Energy harvester (e) Film's SEM images before and after annealing.

Table 1: Implantable devices and their energy consumption [5]

Category	Devices	Voltage needed (V)	Power consumption
Biosensors	Biosensor timers	0.3-1.3	< 660 pW
	ADC conversion.	1.2-1.5	< 35 µW
Communications	Radiofrequency transmitting devices	0.5-1.2	10 µW to 1.5 mW
	Ultrasonic transducers.	0.5-2.0	0.5-1.5 mW
Stimulations	Electrical stimulations	1.6-3.0	1 µW to 25 mW
	Actuators	4.0-4.5	50-100 mW

2. Design and Fabrication

Figure. 1 presents a cross-sectional SEM image of the actual device, showcasing its layered configuration. The 1 cm^2 device possesses a micrometre scale thickness, making it highly flexible. The schematic of the device structure is depicted in Fig. 2b. The core component is a piezoelectric P(VDF-TrFE) free-standing film, flanked by gold (Au) and chromium (Cr) electrodes.

To fabricate the thin film, PVDF-TrFE (75:25 mol%) powder was dissolved in N, N-dimethylformamide (DMF, 99.8 vol%) at a 15 wt% concentration. The solution was ultrasonic stirred for two 30-minute intervals to ensure thorough dissolution. In the second step, this solution was spin-coated onto a glass substrate. It has been observed in recent research that the remnant polarization, crystallinity, dielectric constant, and Young's modulus are directly affected by the spin coating conditions in the case of P(VDF-TrFE) based nanogenerators [35]. The effects can be attributed to the centrifugal force-induced shear stress and grain alignments. In addition, the rotational speed is directly proportional to Young's modulus, which itself is inversely proportional to the piezoelectric power [36]. Hence, the process was carried out in two steps – 500 rpm for 10 seconds and 2000 rpm for 40 seconds – to obtain a 20 µm thick film.

Subsequently, the device underwent annealing. Temperature greatly influences crystallinity, while the optimal range lies between the Curie temperature (120 °C) and melting temperature (150 °C) [37][38]. Moreover, the paraelectric phase allows for a better crystallinity ratio (up to 91%), and higher crystallinity results in enhanced remnant polarization. Therefore, the PVDF-TrFE film on a glass substrate was annealed at 120 °C for 30 minutes. It has been observed that the annealing greatly enhanced the quality while reducing the surface roughness. The SEM images of the film before and after annealing are shown in Fig. 2(d).

Due to the film's delicate nature and to ensure smooth detachment from the glass substrate, it was subjected to the cold ionized aqua bath for 2 seconds. The free-standing film was then carefully peeled off from the substrate. Next, 10 nm chromium (Cr) and 70 nm gold (Au) electrodes were deposited on each side using physical vapor deposition (PVD), i.e., thermal evaporation at 1500 °C.

The final step involved the electrical polarization of the device. The objective was to apply a strong electric field across the electrodes to align dipoles. In this case, 450 Vμm^{-1} was applied for 10 seconds along the thickness mode of the energy harvester. During the poling process, the intensity of the electric field is more critical than the poling duration in determining effectiveness [38]. Furthermore, the poling direction directly impacts the output from the device; when parallel to the applied stress, the material operates in the d_{33} mode, resulting in a high coupling coefficient and, consequently, a high power output [39][40]. The step-by-step fabrication procedure and the poling direction are shown in Fig. 2a and Fig.2c respectively.

To ascertain the output yield of the device, section 4 provides a detailed description of the device's testing and characterization within multiple mediums.

3. Experimental Results and Discussion

The energy harvesting performance of the device was evaluated using a customized PCB-board testing platform in three different mediums – water, and animal meat tissue to gauge the performance in dense mediums; while in the air for an enhanced understanding of the behaviour; as shown in Fig. 4. The edges of the device were fixed onto the PCB board using a metal washer while connecting the two electrodes to the oscilloscope. To excite the IUEH, an external bulk-mode ultrasonic wave transmitter (Tx) powered by an FPA-1016 amplifier and a waveform generator was employed. A wide frequency sweep ranging from 20 kHz to 1 MHz was applied, and the power output was measured using a variable resistor (10 kΩ - 200 kΩ), while the voltage across the device was observed with an oscilloscope. As piezoelectric energy harvesting involves the conversion of mechanical acoustic signal to electricity, optimal energy conversion is achieved when the device operates at its resonant frequency; since the output of the device is directly proportional to the induced stress within the piezoelectric material. Therefore, a finite element analysis (FEA) was done using Comsol Multiphysics for resonant frequency simulation of the IUEH with solid mechanics and electrostatic interface. Frequency sweep analysis was done to simulate the device from 20 kHz to 1 MHz with a step of 20 kHz, as shown in Fig. 3(b). In this, the physics-controlled normal mesh is used for simplification. As part of the boundary conditions, all four edges of the device were anchored. The physical properties of the materials used during the simulation are provided in Table 2. Resultantly, the peak was obtained at 80KHz. Further refinement was done using eigenfrequency analysis (Fig. 3(a)), revealing a resonance frequency precisely to be around 82.1 KHz. The subsequent experimentation further substantiated the simulation results when the device yielded maximum output at the frequency of 80 kHz.

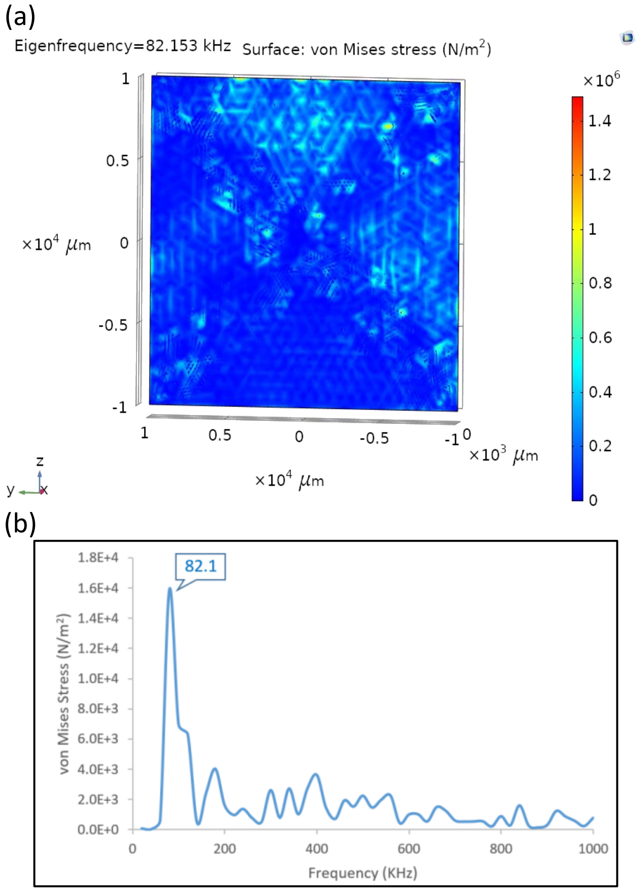

Figure 3: (a) Resonance Frequency in Comsol Simulation. (b) Frequency sweep analysis from 20KHz to 1MHz

Table 2: Parameters of P(VDF-TrFe) used in Comsol[41].

Parameters	P(VDF-TrFE)(75:25)[57,59,60]
Density	1874
Young's modulus Y (GPa)	1.1-3
Dielectric constant (ε_r)	12
Dielectric loss (tanδ_e)	0.018
Mechanical loss (tanδ_m)	0.05
d_{33} (pC N^{-1})	24-38
d_{31} (pC N^{-1})	6-12
k_{33}	0.37
k_{31}	0.07
Poisson ratio	0.33
	Gold (Au) Electrodes
Young's Modulus (GPa)	70
Poisson ratio	0.44
Density (kg/m^3)	19300
Thickness (nm)	70

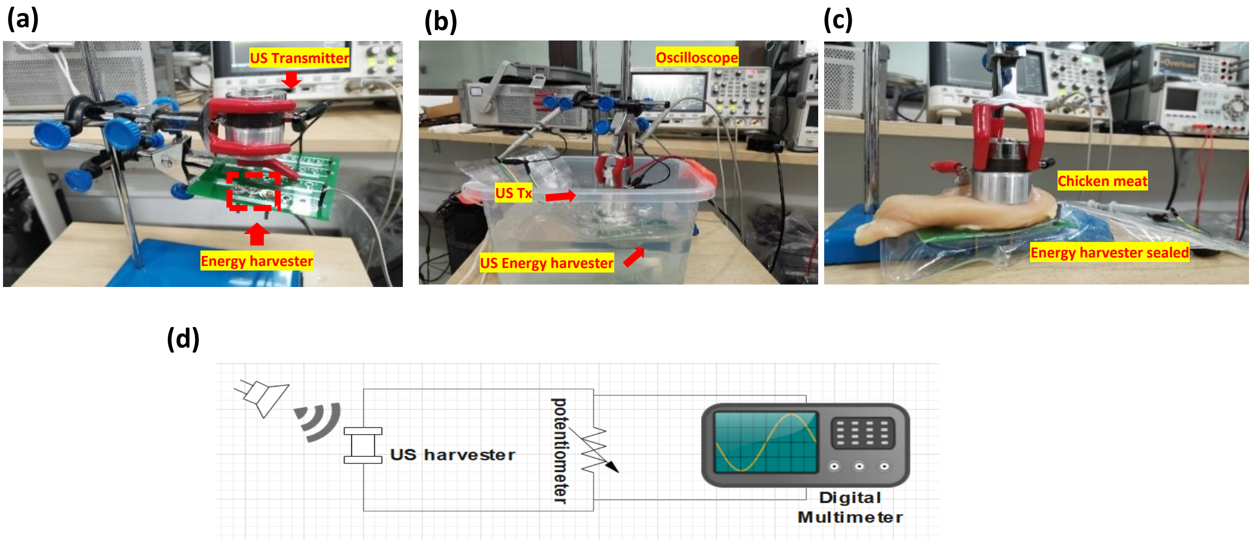

Figure 4: Testing of US energy harvester in (a)Air, (b)Water, and (c)Animal meat; (d) circuitry configuration for power output.

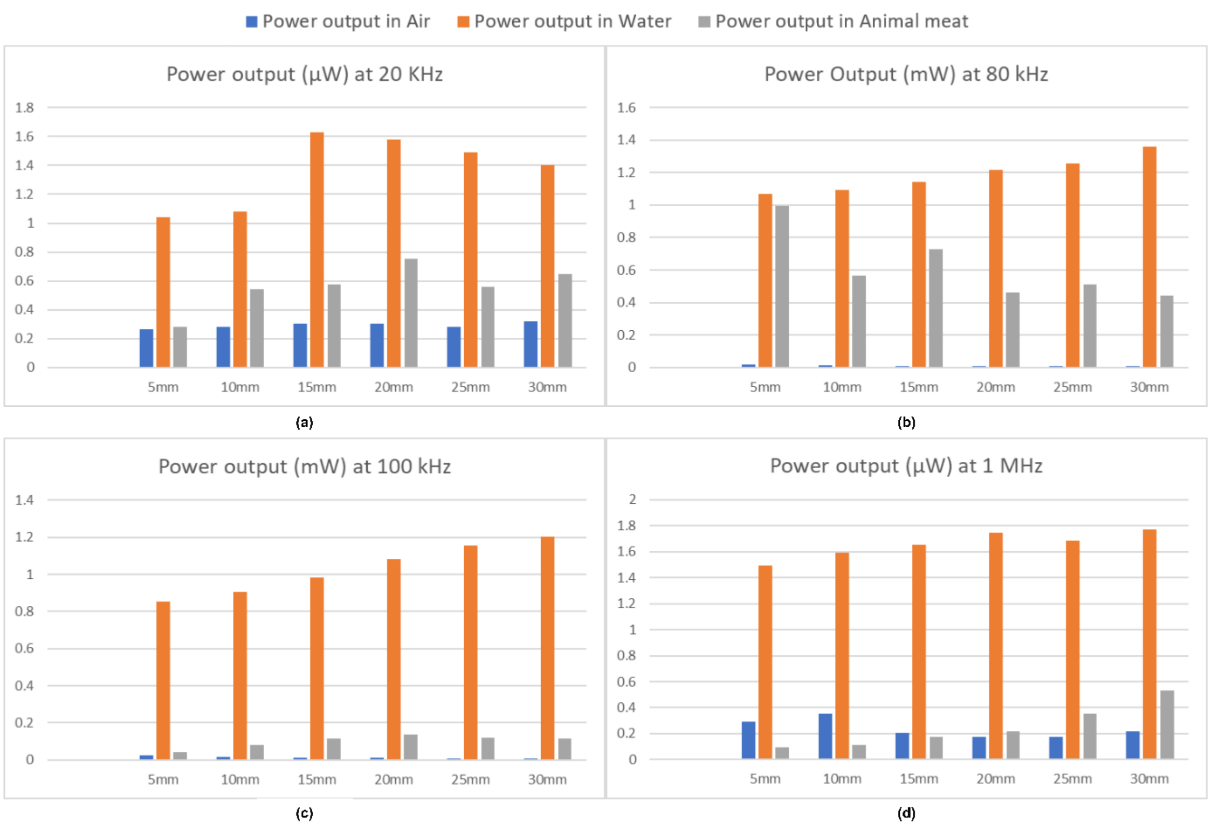

Figure 5: Energy harvester output in Air, water and animal meat at four different Transmitter frequencies

Performance in Air:

The experimental performance evaluation of the IUEH involved fixing it onto an apparatus, as shown in Fig 4(a-c). The ultrasound transmitter (Tx) was positioned at varying distances from the energy harvester, to observe the proportionality of the device's output in each case. For a better understanding, the output of the device without packaging in air was investigated, which is minimal due to the medium's low density. The device exhibited a maximum output power of 17 µW and a voltage of 860 mV at a 5 mm distance from the Tx. The output decreased as the distance increased; finally, reaching 10 µW and 550 mV at 30 mm, as illustrated in Fig. 5 (a-d).

Performance in Water:

To gauge the output of the device in a denser medium, it is submerged in water by enclosing in a very thin waterproof PVC plastic bag – while aiming to keep minimum attenuation. Here, a maximum power generation of 1.4 mW and a potential difference of 7 V, at 30 mm/80 kHz frequency is obtained – Fig. 5b. This output is observed because of the inherent low propagation losses of the ultrasonic waves in a denser medium. A graphical illustration of the behaviour of the device at various frequencies can be seen in Fig. 5(a-d).

Performance in Animal Meat:

To evaluate the potential of the ultrasonic energy harvester for use in implantable devices, in-vivo testing was conducted using chicken meat as a model for human tissue, demonstrating the device's ability to generate energy in a simulated biological environment. The device is packaged in a PVC bag and sandwiched within the meat of varying thicknesses, from 5 mm to 30 mm. The Tx is placed on top and excited with a 51 V input signal, as shown in Fig. 4(c). The IUEH, in this case, demonstrated a similar pattern to the water bath testing, since meat also allows better propagation due to high density. The maximum output of 1.1 mW and 4 V at 80 kHz (5 mm) is obtained (Fig. 5b).

Discussion:

The variation in the output signal with respect to the distance between the transmitter probe and the receiver is believed to arise from (a) maxima and minima of the ultrasonic signal, and (b) misalignment or alignment between the two devices [42]. Additionally, the operating environment – air, water bath, or tissue- influences the power transfer efficiency.

To assess the efficiency of the energy harvester, the ratio of power output to power input, represented as efficiency (η), is calculated. Efficiency is a crucial metric indicating the effectiveness of the energy harvester in converting ultrasound energy into usable electrical power. The formula for efficiency is given by:

$$\eta = \left(\frac{V_{output}}{V_{input}}\right) \times 100\%$$

V_{output} is the peak-peak voltage obtained from the energy harvester, and V_{input} is the peak-peak voltage applied to the ultrasound transmitter. Keeping the input voltage to the US transmitter at 51 V, the efficiency of the energy harvester stands at 1.56%, 12.73%, and 7.27% in Air, Water, and Animal meat, respectively. This value signifies the proportion of the input ultrasound energy effectively transformed into electrical power by the energy harvester.

In addition, the resonance frequency of the surrounding medium plays an important part. For instance, Air being less dense, possesses a lower acoustic impedance compared to denser materials like water and meat which can result in intermittent energy transfer. On the other hand, in denser media like water and meat, where the acoustic impedance is higher, the harvester's resonance frequency of 80 kHz aligns correctly with the medium's properties. This alignment facilitates effective energy transfer and enhances the harvester's mechanical response, resulting in higher output voltages at the resonance frequency in water and meat. As a result, the device demonstrated remarkable power output within the optimal range for powering implantable devices. Detailed analysis and comparison with the peer devices are given in Table 3.

4. Conclusion

In conclusion, this study presents a promising approach for wireless energy harvesting using a high-frequency implantable energy harvester (IUEH) based on P(VDF-TrFE). The use of biocompatible material and a simple fabrication process, including spin coating, thermal evaporation, and DC-polarization, make this device highly suitable for implantable medical devices. Both theoretical and experimental measurements demonstrate that the projected resonance frequencies of close to 80 kHz from Comsol simulations align perfectly with the practical measurements, where the output peaks. The 1 cm^2 IUEH generated peak output powers of 1.4 mW in water and 1.1 mW within animal meat. These results suggest that the proposed device has great potential as a wireless energy source for simple implantable medical devices such as pacemakers, stimulators, and biosensors. Future work will focus on optimizing the device design and exploring its potential for more complex applications.

Acknowledgements

This research was supported by the National Natural Science Foundation of China (No. 62074040) and the Natural Science Foundation of Shanghai (No. 20ZR1404000).

Ethical source of Experimenting material:

The meat used in this research was obtained from a commercial source.

Table 3: Piezoelectric implantable energy harvesters reported in literature.

Material	Fabrication Technique(s)	Substrate	Excitation	Power Density	Output Voltage	Reference
PVDF-TrFE	Photolithography, Etching, Spin coating, Magnetron sputtering, Thermal evaporation	Silicon (300 μm)	6.6-19.8 kHz	N/A	23-29 μV	Inaoka et al. [16]
PVDF-TrFE layer, Silver polymer paste electrodes	Screen printing, Drop casting	Polyethylene terephthalate (PET: Melinex)	0.2 N-0.7 N load	9.08×10^{-2} mW/cm^2	3.06 V	KK. Chow et al. [43]
PZT, Silver paste, Copper	Sputtering, Curing	PDMS	200-500 kHz	14.1 mW/cm^2	1.2 V	L.Jiang et al. [18]
PZT-5A	N/A	N/A	24.4 kHz	N/A	5.8 Vpp	T.Li et al. [19]
KNNS/epoxy 1-3 Piezocomposite, Cr/Au and Copper electrode,	Solid state sintering, sputtering	Silicon Elastomer	300 kHz	4.1×10^{-3} mW/cm^2	~1.4 Vpp	L.Jiang et al. [20]
Bottom and top Pt electrodes, PZT	Sputtering, DC magnetron sputtering, sol-gel process, etching, DRIE	Si, SiO_2	100 kHz-1 MHz	3.75×10^{-3} mW/cm^2	2 mV	Q.Shi et al. [21]
Ti/Pt, PZT, silver epoxy, PDMS, CSO Selenium, parylene	PECVD, laser micromachining, etching	Glass wafer	2.3 MHz	N/A	7 V	T. Maleki et al. [22]
PZT, copper, conductive epoxy	N/A	N/A	1 MHz	N/A	1 V	J.Charthad et al. [23]
Silicon, Cr/Au, Silica, Photoresist, PZT	Sputtering, Bonding and Thinning, Patterning, Etching	Silicon Oxide	40.43 kHz	38 mW/cm^3	1.24 V	Q.He et al. [44]
PVDF-TrFE, Cr/Au	**Spin coating, PVD, DC Polarization**	**No substrate**	**20 kHz-1 MHz**	1.1 mW/cm^2	**7 V (Water)/ 4 V (Animal meat)**	**This work**

References

[1] Safaei M, Meneghini R M and Anton S R 2018 Force detection, center of pressure tracking, and energy harvesting from a piezoelectric knee implant *Smart Mater. Struct.* **27** 114007

[2] Edwards S J, Wakefield V, Jhita T, Kew K, Cain P and Marceniuk G 2020 Implantable cardiac monitors to detect atrial fibrillation after cryptogenic stroke: a systematic review and economic evaluation *Health Technol. Assess. (Rockv).* **24** v–184

[3] Jiang L, Yang Y, Chen R, Lu G, Li R, Xing J, Shung K K, Humayun M S, Zhu J, Chen Y and Zhou Q 2019 Ultrasound-Induced Wireless Energy Harvesting for Potential Retinal Electrical Stimulation Application *Adv. Funct. Mater.* **29** 1902522

[4] Swann N C, De Hemptinne C, Thompson M C, Miocinovic S, Miller A M, Gilron R, Ostrem J L, Chizeck H J and Starr P A 2018 Adaptive deep brain stimulation for Parkinson’s disease using motor cortex sensing *J. Neural Eng.* **15**

[5] Jiang L, Yang Y, Chen Y and Zhou Q 2020 Ultrasound-induced wireless energy harvesting: From materials strategies to functional applications *Nano Energy* **77** 105131

[6] Arra S, Leskinen J, Heikkilä J and Vanhala J 2007 Ultrasonic power and data link for wireless implantable applications *2007 2nd Int. Symp. Wirel. Pervasive Comput.* 567–71

[7] Amar A Ben, Kouki A B and Cao H 2015 Power approaches for implantable medical devices *Sensors (Switzerland)* **15** 28889–914

[8] Hannan M A, Mutashar S, Samad S A and Hussain A 2014 Energy harvesting for the implantable biomedical devices: issues and challenges *Biomed. Eng. Online* **13** 79

[9] Lau E W 2017 Technologies for Prolonging Cardiac Implantable Electronic Device Longevity *Pacing Clin. Electrophysiol.* **40** 75–96

[10] McAuley J, Farah N, Van Gröningen R and Green C 2013 A Questionnaire-Based Study on Patients’ Experiences

with Rechargeable Implanted Programmable Generators for Spinal Cord Stimulation to Treat Chronic Lumbar Spondylosis Pain *Neuromodulation Technol. Neural Interface* **16** 142–6
[11] Materials S 2016 A Review of Acoustic Power Transfer for Bio- Medical Implants 0–24
[12] Wei X and Liu J 2008 Power sources and electrical recharging strategies for implantable medical devices **2** 1–13
[13] Kim S, Choi S J, Zhao K, Yang H, Gobbi G, Zhang S and Li J 2016 Electrochemically driven mechanical energy harvesting *Nat. Commun. 2016 71* **7** 1–7
[14] Taalla R V., Arefin M S, Kaynak A and Kouzani A Z 2019 A review on miniaturized ultrasonic wireless power transfer to implantable medical devices *IEEE Access* **7** 2092–106
[15] Chang T C, Weber M J, Wang M L, Charthad J, Khuri-Yakub B T and Arbabian A 2016 Design of Tunable Ultrasonic Receivers for Efficient Powering of Implantable Medical Devices With Reconfigurable Power Loads *IEEE Trans. Ultrason. Ferroelectr. Freq. Control* **63** 1554–62
[16] Inaoka T, Shintaku H, Nakagawa T, Kawano S, Ogita H, Sakamoto T, Hamanishi S, Wada H and Ito J 2011 Piezoelectric materials mimic the function of the cochlear sensory epithelium *Proc. Natl. Acad. Sci. U. S. A.* **108** 18390–5
[17] Chow K K, Abdal-Kadhim A M, Kok S L and Lau K T 2019 Finite elements method simulation of P(VDF-TrFE) piezoelectric sensor for Internet of things application *Int. J. Integr. Eng.* **11** 77–83
[18] Jiang L, Yang Y, Chen R, Li R, Li D, Humayun M S, Kirk K, Zhu J, Chen Y, Zhou Q, Jiang L, Yang Y, Chen R, Lu G, Li D, Humayun M S, Shung K K, Zhu J and Chen Y 2018 Author ' s Accepted Manuscript Flexible piezoelectric ultrasonic energy harvester array for bio-implantable wireless generator Reference : To appear in : Nano Energy
[19] Li T and Lee P S 2019 Piezoelectric Energy Harvesting with an Ultrasonic Vibration Source
[20] Jiang L, Yang Y, Chen R, Lu G, Li R, Xing J, Shung K K, Humayun M S, Zhu J, Chen Y and Zhou Q 2019 Ultrasound-Induced Wireless Energy Harvesting for Potential Retinal Electrical Stimulation Application *Adv. Funct. Mater.* **29** 1–13
[21] Shi Q, Wang T and Lee C 2016 MEMS Based Broadband Piezoelectric Ultrasonic Energy Harvester (PUEH) for Enabling Self-Powered Implantable Biomedical Devices *Sci. Rep.* **6** 1–10
[22] Maleki T, Cao N, Song S H, Kao C, Arthur Ko S C and Ziaie B 2011 An ultrasonically powered implantable Micro-Oxygen generator (IMOG) *IEEE Trans. Biomed. Eng.* **58** 3104–11
[23] Charthad J, Weber M J, Chang T C and Arbabian A 2015 A mm-Sized Implantable Medical Device (IMD) With Ultrasonic Power Transfer and a Hybrid Bi-Directional Data Link *IEEE J. Solid-State Circuits* **50** 1741–53
[24] Yu C, Xu J, Yang L, Ye M, Ye Y, Li T, Zhang Y, Zhang Z, Xu H, Tan H, Zhang G and Zhang H 2023 Self-driving flexible piezoresistive sensors integrated with enhanced energy harvesting sensor of ZnO/Ti3C2Tx nanocomposite based on 3D structure *J. Alloys Compd.* **956** 170358
[25] He Q, Li X, Zhang H, Briscoe J, He Q, Li X, Zhang H and Briscoe J 2023 Nano-Engineered Carbon Fibre-Based Piezoelectric Smart Composites for Energy Harvesting and Self-Powered Sensing *Adv. Funct. Mater.* **33** 2213918
[26] Kulkarni N D and Kumari P 2023 Role of rGO on mechanical, thermal, and piezoelectric behaviour of PVDF-BTO nanocomposites for energy harvesting applications *J. Polym. Res.* **30** 1–17
[27] Sadl M, Nadaud K, Bah M, Levassort F, Eckstein U, Khansur N H, Webber K G and Ursic H 2022 Multifunctional energy storage and piezoelectric properties of 0.65Pb(Mg1/3Nb2/3)O3–0.35PbTiO3 thick films on stainless-steel substrates *J. Phys. Energy* **4** 024004
[28] Matova S P, Renaud M, Jambunathan M, Goedbloed M and Van Schaijk R 2013 Effect of length/width ratio of tapered beams on the performance of piezoelectric energy harvesters *Smart Mater. Struct.* **22**
[29] Guo S, Duan X, Xie M, Aw K C and Xue Q 2020 Composites, Fabrication and Application of Polyvinylidene Fluoride for Flexible Electromechanical Devices: A Review *Micromachines* **11** 1–29
[30] Ramadan K S, Sameoto D, Evoy S, Ramadan K S, Sameoto D and Evoy S 2014 A review of piezoelectric polymers as functional materials for electromechanical transducers *SMaS* **23** 033001
[31] Shabara M A, Badawi A R and Xu T B 2020 Comprehensive piezoelectric material application issues on energy harvesting for artificial intelligence systems *AIAA Scitech 2020 Forum* **1 PartF**
[32] Marin A, Bressers S and Priya S 2011 Multiple cell configuration electromagnetic vibration energy harvester *J. Phys. D. Appl. Phys.* **44**
[33] Agarwal K, Jegadeesan R, Guo Y X and Thakor N V. 2017 Wireless Power Transfer Strategies for Implantable Bioelectronics *IEEE Rev. Biomed. Eng.* **10** 136–61
[34] Palosaari J, Leinonen M, Juuti J, Hannu J and Jantunen H 2014 Piezoelectric circular diaphragm with mechanically induced pre-stress for energy harvesting *Smart Mater. Struct.* **23**
[35] Chang J 2019 Spin Coating Epitaxial Films *Cailiao Daobao/Materials Reports* **33** 1919–20
[36] Jeong D G, Singh H H, Kim M S and Jung J H 2023 Effect of Centrifugal Force on Power Output of a Spin-Coated Poly(Vinylidene Fluoride-Trifluoroethylene)-Based Piezoelectric Nanogenerator *Energies* **16** 1892
[37] Ahmad N, Majid W H A, Zaini M S, Rosli A K, Adnan R H and Halim N A 2023 Energy harvesting performance of a novel polymer-nanocrystal composite of P(VDF-TrFE)/ZnO QD films *Mater. Sci. Eng. B* **289** 116256
[38] Ducrot P H, Dufour I and Ayela C 2016 Optimization of PVDF-TrFE Processing Conditions for the Fabrication of Organic MEMS Resonators *Sci. Rep.* **6** 1–7
[39] Wang Z, Maruyama K and Narita F 2022 A novel manufacturing method and structural design of functionally graded piezoelectric composites for energy-harvesting *Mater. Des.* **214** 110371
[40] Christensen D B and Roundy S 2016 Ultrasonically powered piezoelectric generators for bio-implantable sensors: Plate versus diaphragm *J. Intell. Mater. Syst. Struct.* **27** 1092–105
[41] Anon 2002 Encyclopedia of Polymer Science and Technology *Encycl. Polym. Sci. Technol.*
[42] Chang T C, Wang M L, Charthad J, Weber M J and Arbabian A 2017 A 30.5mm3 fully packaged implantable device with duplex ultrasonic data and power links achieving 95kb/s with <10-4 BER at 8.5cm depth *Digest of Technical Papers - IEEE International Solid-State Circuits*

Conference vol 60 (Institute of Electrical and Electronics Engineers Inc.) pp 460–1
[43] Chow K, Kok S and Lau K 1843 Design and Characterization of Piezoelectric P (VDF-TrFE) Thick Film on Flexible Substrate for Energy Harvesting **10** 63–8
[44] He Q, Liu J, Yang B, Wang X, Chen X and Yang C 2014 MEMS-based ultrasonic transducer as the receiver for wireless power supply of the implantable microdevices *Sensors Actuators, A Phys.* **219** 65–72